Published in final edited form as:
Neuroimage. 2013 February 1; 0: 508–521. doi:10.1016/j.neuroimage.2012.10.013.

Nucleus accumbens, thalamus and insula connectivity during incentive anticipation in typical adults and adolescents☆,,☆☆

Youngsun T. Cho[a], **Stephen Fromm**[b], **Amanda E. Guyer**[c], **Allison Detloff**[b], **Daniel S. Pine**[b], **Julie L. Fudge**[a], and **Monique Ernst**[b,*]

[a]Department of Neurobiology and Anatomy, University of Rochester Medical Center, NY, USA

[b]Section on Development and Affective Neuroscience Branch, National Institute of Mental Health, NIH, DHHS, MD, USA

[c]Center for Mind and Brain, University of California, Davis, CA, USA

Abstract

Reward neurocircuitry links motivation with complex behavioral responses. Studies of incentive processing have repeatedly demonstrated activation of nucleus accumbens (NAc), thalamus, and anterior insula, three key components of reward neurocircuitry. The contribution of the thalamus to this circuitry in humans has been relatively ignored, a gap that needs to be filled, given the central role of this structure in processing and filtering information. This study aimed to understand how these three regions function as a network during gain or loss anticipation in adults and youth. Towards this goal, functional magnetic resonance imaging (fMRI) and dynamic causal modeling (DCM) were used to examine effective connectivity among these three nodes in healthy adults and adolescents who performed the monetary incentive delay (MID) task. Seven connectivity models, based on anatomic connections, were tested. They were estimated for incentive anticipation and underwent Bayesian Model Selection (BMS) to determine the best-fit model for each adult and adolescent group. Connection strengths were extracted from the best-fit model and examined for significance in each group. These variables were then entered into a linear mixed model to test between-group effects on effective connectivity in reward neurocircuitry. The best-fit model for both groups included all possible anatomic connections. Three main findings emerged: (1) Across the task, thalamus and insula significantly influenced NAc; (2) A broader set of significant connections was found for the loss-cue condition than the gain-cue condition in both groups; (3) Finally, between-group comparisons of connectivity strength failed to detect statistical differences, suggesting that adults and adolescents use this incentive-processing network in a similar manner. This study demonstrates the way in which the thalamus and insula influence the NAc during incentive processing in humans. Specifically, this is the first study to demonstrate in humans the key role of thalamus projections onto the NAc in support of reward processing. Our results suggest that anticipation of gain/loss involves an

☆Funding: F30 MH091926-02 (YTC); Intramural Research Program-NIMH.

☆☆None of the authors have any conflict of interest.

*Corresponding author at: Emotional Development and Affective Neuroscience Branch (EDAN), National Institute of Mental Health, National Institutes of Health, 15K North Drive, Bethesda, MD 20892, USA. Fax: +1 301 402 2010. ernstm@mail.nih.gov (M. Ernst).

'alerting' signal (thalamus) that converges with interoceptive information (insula) to shape action selection programs in the ventral striatum.

Introduction

Reward neurocircuitry consists of a distributed neural network that translates motivation into motor responses (Haber and Knutson, 2010; Robbins and Everitt, 1996). Within this network, meta-analyses of reward processing in functional magnetic resonance imaging (fMRI) studies demonstrate consistent activation within the nucleus accumbens (NAc), thalamus, and insula cortex (meta-analyses: Knutson and Greer, 2008; Liu et al., 2011). These studies have reported similar Activation Likelihood Estimate (ALE) scores for all three regions within an order of magnitude during gain anticipation vs loss anticipation, and gain anticipation vs. gain outcome (meta-analysis:(Knutson and Greer, 2008)), as well as similar Parametric Voxel-based Meta-Analysis (PVM) scores for the three regions during reward anticipation (meta-analysis: Liu et al., 2011). While other regions such as orbitofrontal (OFC) and medial prefrontal cortices are involved in reward processing, the size and varied functions within sub-areas of these regions has made it difficult to assign an explicit role to specific coordinates in independent studies (Duncan and Owen, 2000; Gilbert et al., 2010). Instead, the NAc, thalamus, and anterior insula are smaller, discrete regions that demonstrate a likelihood of increased blood oxygen level dependent (BOLD) signal activations during reward processing similar to other regions such as the amygdala and OFC (meta-analysis: Liu et al., 2011). The consistency and strength of these activations make these regions ideal for connectivity analyses requiring strongly activated regions, such as dynamic causal modeling (DCM) (Friston et al., 2003). Surprisingly, despite its central position within the basal ganglia loops, the thalamus has largely been ignored in functional imaging analyses of reward anticipation. The use of DCM to measure how these regions influence one another as a network is particularly suitable, given the classic non-human primate studies demonstrating anatomic interconnections among these three regions (Chikama et al., 1997; Gimenez-Amaya et al., 1995; Haber et al., 1990; Mufson and Mesulam, 1984). This focus on connectivity among these three structures, particularly the thalamus, represents a novel contribution of this work.

The NAc is at the core of the reward system, as it integrates emotional information to modulate motivated behavior (Mogenson et al., 1980; Roesch et al., 2009). Accordingly, fMRI studies repeatedly report increased BOLD signal activation of the NAc in response to rewards vs. losses (Breiter et al., 2001; Cooper and Knutson, 2008; Delgado et al., 2000; Knutson et al., 2001), but see (Jensen et al., 2003; Zink et al., 2003). The NAc receives inputs from many regions, among which the thalamus and anterior insula occupy key positions; in turn, thalamus and anterior insula project to one another (Fig. 1) (Chikama et al., 1997; Gimenez-Amaya et al., 1995; Groenewegen and Berendse, 1994; Van der Werf et al., 2002). In addition, meta-analysis has shown that spontaneous activity in the NAc predicts activity in other reward regions, including the thalamus and insula, suggesting consistent co-activation among these three regions (meta-analysis: Cauda et al., 2011).

The midline thalamus is strongly modulated by the ascending reticular activating system and therefore plays an important 'alerting' role in salience detection (Matsumoto et al., 2001). Through its massive projections to the striatum, the midline thalamus drives attentional and behavioral shifts to changing external cues (Smith et al., 2011). One hypothesis is that the thalamostriatal pathway stimulates cholinergic neurons, creating a substrate for suppression of ongoing motor activity in the face of salient external stimuli (Ding et al., 2010). As such, this function is critical to adjust behavior to incentives. Accordingly, meta-analyses of fMRI studies also demonstrate consistent activation of the thalamus in studies of reward processing in the context of both gains and losses (meta-analyses: Knutson and Greer, 2008; Liu et al., 2011). Adolescents also demonstrate increased thalamic activation, or significant effects of age on thalamic activation, during reward processing (Bjork et al., 2004, 2010; Christakou et al., 2011; Cohen et al., 2010; Van Leijenhorst et al., 2010a,b), a finding that may be related to changes in thalamic grey-matter volume and white-matter tract organization in children and adolescents (Asato et al., 2010; Barnea-Goraly et al., 2005; Group, 2012; Hasan et al., 2011; Sowell et al., 2002).

The anterior insula also integrates multiple sensory modalities from the brainstem, including visceral, autonomic and somatosensory information. Only in higher primates are these interoceptive cues relayed by the ventromedial nucleus of the thalamus (Craig, 2002). The anterior half of the insula also receives exteroceptive cues from the amygdala (Mufson et al., 1981; Nishijo et al., 1988). The convergence of exteroceptive and vegetative inputs leads to the notion that the insula processes 'interoceptive awareness', or a continuous sense of the 'sentient self' (Craig, 2009; Nieuwenhuys, 2012). Therefore, the projections from the insula to the NAc are expected to critically influence motivated behavior, particularly decision-making (Clark et al., 2008; Damasio, 1999; Naqvi and Bechara, 2009). Finally, the NAc integrates the information from the insula and the thalamus into motivational processes, and this processed information is then output back to the thalamus, either directly, or mostly indirectly via the globus pallidus, feeding basal-ganglia loops to shape behavior (Haber et al., 1990; rev: Haber 2003).

Collectively, data on anatomic interconnections, together with the strong pattern of fMRI activation in reward tasks, support the notion that the NAc, thalamus, and insula function as a unit to influence incentive processing through mutual interactions. A few studies have used DCM to understand how a network operates in response to incentives, demonstrating the involvement of NAc and cortical connections during reward processing (Alexander and Brown, 2010; Gonen et al., 2012; Veldhuizen et al., 2011). These studies highlight not only the pattern of functional links among other key structures in a reward context, but also raise the additional question of how incentive valence (e.g., gain vs. loss) influences this functional pattern, and within a wider network. In addition, a developmental perspective, particularly across adolescence, has enormous relevance given the adolescent peak vulnerability for substance use problems, which implicates these same structures (Gu et al., 2010; Jia et al., 2011).

To address these questions, the present study uses the well-published monetary incentive delay (MID) task (Knutson et al., 2001) in conjunction with dynamic causal modeling (DCM) to quantify the effects of monetary gain and loss anticipation on direction-specific

effective connectivity (Friston et al., 2003). Effective connectivity models the influence of one brain region on another (Friston et al., 2003). As such, DCM builds upon a traditional general linear model (GLM) analysis by modeling the effective connectivity of activated regions, thereby requiring regions of interest that are strongly activated by the task at hand (Stephan et al., 2010). The three regions selected for the DCM analysis, NAc thalamus and insula, are all consistently activated by the MID task (Bjork et al., 2004; Knutson and Greer, 2008; Knutson et al., 2001; Samanez-Larkin et al., 2007). In addition, this task has been previously examined in two studies comparing adults and adolescents, allowing us to extend previous findings (Bjork et al., 2004, 2010). While demonstrating relative hypoactivation of the ventral striatum during reward anticipation in adolescents compared to adults, both studies reported that the adolescent and the adult groups independently exhibited robust activation to the MID task, making it ideal for a DCM study (Bjork et al., 2004, 2010).

The goal of this work is to examine how cue-elicited incentive anticipation modulates anatomically relevant connections within a core incentive-processing network in adults and adolescents. We hypothesize that: 1. connections among the thalamus, NAc and insula would reveal an incentive processing neural network, which, based on the above basic-science review, would exhibit the strongest links for thalamus-to-NAc, insula-to-NAc, and thalamus-to-insula connections; 2. based on studies reporting differential BOLD activation patterns in response to incentive valence (Hardin and Ernst, 2009; Tom et al., 2007), the network would be modulated distinctly by gains and losses, with a stronger implication of insula connections in losses than gains, and NAc connections in gains than losses; 3. finally, based on developmental resting-state functional connectivity work (Fair et al., 2008; Kelly et al., 2009; Stevens et al., 2009), adolescents would demonstrate weaker effective connectivity in this network than adults.

Methods

Subjects

Thirty healthy adults, aged 22–48 years (mean 28.8±7.5 years; 11 males and 19 females), and twenty-four healthy adolescents, aged 10–17 years (mean 14.6±2.0 years; 15 males and 9 females), were recruited locally through advertisements. Groups did not differ significantly on sex, socioeconomic status, or handedness. However, IQ was significantly higher ($t=3.4$, $df=52$, $p=0.001$) in adults (mean 120.8±10.6) than adolescents (mean 110.4±11.9), and was thus used as a covariate of nuisance in fMRI analyses. Physical and mental health was confirmed by medical history, physical examination, and administration of the Kiddie Schedule for Affective Disorders and Schizophrenia—Present and Lifetime version (K-SADS-PL) (Kaufman et al., 1997) for adolescents or the Structured Clinical Interview for DSM-IV (SCID) (Spitzer et al., 1992) for adults. Exclusion criteria included a history of psychiatric illness or head injury, neurological disorders, exposure to traumatic life events, use of a psychoactive substance or inability to complete the fMRI scan (e.g., those with metal implants or claustrophobia). All methods were approved by the institutional review board of the National Institute of Mental Health (Bethesda, MD). After being explained the study, adult participants and parents of minors signed a consent form, and adolescents signed an assent form.

MID task

The event-related MID task probes anticipation and response to visual cues representing forthcoming monetary rewards or losses (Knutson et al., 2001). The entire task was composed of two runs of 72 trials each, with each trial lasting 6 s. Each trial began with a 250 ms cue indicating the amount of potential reward or loss, followed by a fixation period (2000–2500 ms), and a response target (160–250 ms) (Fig. 2). Subjects were asked to press a button as quickly as possible during the response target presentation, in order to win, or avoid losing, money. Following the disappearance of the target, subjects received feedback for 1650 ms indicating the outcome of the trial, and their cumulative dollar amount. Consistent with the original MID task, the inter-trial interval (ITI) was jittered between 1350 and 1940 ms. This relatively short ITI has raised questions regarding the efficiency of the design. A recent study used a modified version of the MID task with longer ITIs (Bjork et al., 2010) and showed similar results to the past work with a shorter ITI design (Bjork et al., 2004), suggesting reasonable stability in activation patterns, independent of the ITI length. In addition, the original version of the MID task that we employed has been used in far more published studies than the version with variable-duration ITI, allowing the present study to extend previous findings.

Circle cues represented the potential for monetary gain (presented 64 times total, across both runs), square cues indicated the potential for losses (presented 64 times total, across both runs), and triangle cues represented no money to be won or lost (presented 16 times total, across both runs). The amount of reward or loss was represented by one line drawn within the shape ($0.20), two lines ($1), or three lines ($5), each shown 32 times across both the circle and square cues. Both circle and square stimuli also included cues without lines (n=32 total). These cues signaled unpredictable values (“surprise” trials), addressing a question of no interest to the present study, and thus were not examined. The order of trials was randomized within each run. Subjects were trained on the task and performed a practice run before the two experimental runs conducted during the functional scans. The length of response target presentation was set such that subjects succeeded two-thirds of the time, with the target duration for the first run selected based on the initial practice run. Five durations (1 = shortest through 5 = longest) of target presentation were defined, and an appropriate duration was selected at the start of each new run, based on participants’ performance of the previous run, in order to achieve a success rate of 66%. For both adults and adolescent groups, most subjects had durations set in the 2 or 3 range.

fMRI scanning

A General Electric (Waukesha, WI) Signa 3 Tesla magnet was used for scanning. Visual stimuli were shown on a screen at the foot of the scanner, and viewed with mirrors mounted at the head coil. Head movement was constrained with foam padding. The functional images were T2-weighted echo-planar images collected with a repetition time (TR) of 2500 ms, an echo time (TE) of 23 ms, and a flip angle of 90°. Images consisted of 30 interleaved, sagittal slices, each 4 mm thick. Voxel dimension was 3.75 mm×3.75 mm×4 mm, matrix size was 64 by 64, and the field of view was 24 cm. The first four acquisitions in each scan series, collected before equilibrium magnetization was reached, were discarded. A T1-weighted anatomical image was collected on each subject using TR=8100 ms, TE=32 ms, flip angle of

15°, and consisted of 124 1 mm thick slices. The matrix size was 256×256, and field of view was 24 cm. Reaction times for button presses were collected on a Cedrus (San Pedro, CA) Lumina response box.

Behavioral data analysis

Accuracy (number of successful button presses), reaction time (time between target presentation and button press), and post-scan ratings (ranging from −5 = dislike very much, to +5 = like very much) of the different cues (Neutral, Gain $0.20, $1 or $5, Lose $0.20, $1 or $5) were included as dependent variables. Each of these three variables was analyzed using a 3-way repeated-measures ANOVA in SPSS 18 (SPSS, Chicago, IL), with group as a between-subjects factor, and valence (positive or negative) and magnitude ($0.20, $1 or $5) as within-subject factors. For consistency with the fMRI GLM analysis (see below), the rating for the neutral ($0) cue was covaried with each cue rating. Because of technical difficulties, post-scan ratings were not collected for eight adolescents and one adult, and accuracy counts were not collected for eight adolescents. These subjects were excluded from the respective analyses.

fMRI data analysis

All fMRI data was analyzed with the Statistical Parametric Mapping software, version 8 (SPM8, Wellcome Trust Centre for Neuroimaging, London, UK). All functional images were first slice-time corrected, realigned, and then coregistered to their individual anatomic images. Slice-timing correction was done during preprocessing, and not during DCM analysis, due to the interleaved acquisition sequence. Subjects who moved >4 mm in any direction were eliminated. Coregistered anatomic images were then segmented and normalized to a standard MNI template. Images were then smoothed using an 8 mm full-width half-maximum Gaussian kernel.

General linear model analysis

A whole-brain, voxel-wise general linear model (GLM) for cueelicited anticipation was created for each subject. For each cue type (Neutral; Gain $0.20, $1, or $5; Lose $0.20, $1, or $5), the BOLD response was modeled by convolving a sum of delta functions (one at each cue onset time) with a synthetic hemodynamic response function. A high-pass filter cutoff of 128 s was applied to eliminate slow drift. Vectors of no interest included the “surprise” trials, and were not used in any contrasts. For each subject, three contrasts were computed. These contrasts provided the coordinates for the regions of interest to be used in the DCM analysis. These contrasts included: (1) all gain cues versus neutral cue, (2) all loss cues versus neutral cue, and (3) all cues versus neutral cue. Random-effects analysis was used to enter individual subject contrasts into group-level, voxel-wise, regions of interest (ROI) analyses. For completeness, and to validate that the MID task behaved as expected in our hands, we examined not only our three target regions (NAc, thalamus and insula), but also regions commonly activated in previous MID studies (Bjork and Hommer, 2007; Bjork et al., 2004, 2008, 2010, 2011; Guyer et al., 2006; Knutson et al., 2001; Samanez-Larkin et al., 2007). While different contrasts and groups have been used for different studies, regions were chosen if they were activated in more than three separate MID studies across any contrast and any group. The resulting regions included: putamen (Bjork and Hommer, 2007;

Bjork et al., 2004, 2010; Knutson et al., 2001; Samanez-Larkin et al., 2007); caudate (Bjork et al., 2004; Guyer et al., 2006; Knutson et al., 2001; Samanez-Larkin et al., 2007); amygdala (Bjork et al., 2004, 2008; Guyer et al., 2006; Knutson et al., 2001); mPFC/ACC (Bjork et al., 2004, 2008, 2010, 2011; Knutson et al., 2001; Samanez-Larkin et al., 2007); pre-motor/supplementary-motor/motor cortices (Bjork and Hommer, 2007; Bjork et al., 2004, 2008, 2010; Knutson et al., 2001). Anatomic masks that were hand-drawn from previous studies (caudate, putamen, amygdala, mPFC/ACC; Guyer et al., 2006), or from the Automated Anatomical Labeling (AAL) atlas (motor/premotor cortex; Tzourio-Mazoyer et al., 2002) were searched for peak voxel activations surpassing a small-volume correction of $p<0.05$, family-wise error (FWE).

Dynamic causal modeling

DCM assesses effective connectivity of a priori defined regions by employing either a bilinear or nonlinear mathematical model to understand how experimental manipulations perturb the relationships between regions of interest (Friston et al., 2003; Stephan et al., 2008). DCM uncovers hidden neuronal states and relationships between regions of interest by additionally employing a forward model of how neuronal or synaptic activity leads to a measurable BOLD signal (Friston et al., 2003; Stephan et al., 2010). This model is then inverted by using the BOLD signal to uncover the hidden neuronal states and comment on direction-specific changes in coupling between regions in response to task demands (Friston et al., 2003; Stephan et al., 2010).

Bilinear and nonlinear equations

The bilinear form of DCM models experimental task modulation of inter-regional relationships, while the nonlinear form additionally models how activity in anatomic foci modulates inter-regional relationships (Friston et al., 2003; Stephan et al., 2008). Both forms use the BOLD data to solve for three sets of parameters governing: 1. Endogenous connectivity, the first-order connectivity between regions in the absence of task effect; 2. Modulation of the endogenous connectivity by specific task conditions, here, to either gain or loss cues; 3. Direct inputs, the response of a specific region (called the “driver”) to task demands (here, thalamus, see below for rationale). The nonlinear form includes an additional set of parameters modeling the modulation of the connection between two regions by the activity in a third region (Stephan et al., 2008).

Model space selection

DCM further elucidates the potential mechanisms leading to BOLD activations in traditional GLM analyses (Stephan et al., 2010). Therefore, the selection of regions is guided by BOLD activations seen in GLM results, and narrowed according to *a priori* hypotheses about the functions of the regions of interest. In accordance with this, three regions— NAc, insula, and thalamus—activated in our GLM analysis, as well as in other GLM analyses using this task (Bjork et al., 2004, 2010; Knutson et al., 2001; Samanez-Larkin et al., 2007), were chosen. While other regions, such as orbitofrontal and medial prefrontal cortices, and amygdala, are undoubtedly involved in reward processing, our GLM analysis did not demonstrate activation of these regions in both groups and thus could not be used in the

DCM analysis. All tested models were bound by anatomic constraints based on tract-tracing studies in non-human primates. The models employed different combinations of the following connections: bidirectionally between the thalamus and insula, and between the thalamus and NAc (a small accumbens-medial thalamus projection has been documented and was modeled for completeness), and unidirectionally from insula to nucleus accumbens (Chikama et al., 1997; Gimenez-Amaya et al., 1995; Haber et al., 1990; Mufson and Mesulam, 1984).

All models employed the thalamus as the initial recipient of incoming cue sensory information. The thalamus was chosen as the 'driver' site because of its role in sensory and emotional integration (Groenewegen and Berendse, 1994; Van der Werf et al., 2002), and because the MID task features visual cues that have an associated emotional value (valence and salience). The schematic for all seven tested models is shown in Fig. 3. Each model is comprised of anatomically-relevant connections (see above) between the three selected nodes, thalamus, NAc and insula, based on non-human primate literature. Because little is known about how these three regions interact during reward processing, seven models were hypothesized and entered into Bayesian Model Selection (BMS, below) to determine the best-fit model. All models are therefore iterations based on the fully-connected, anatomically-relevant model, Model 1. Model 2 posits the thalamus as a central processing region, independently communicating with the NAc and insula. Model 3 hypothesizes the NAc as the final receiving site of incentive information from the thalamus and insula. Model 4 is a closed-loop model based on the striato-thalamo-cortico-striatal loop model. Models 5 and 6 posit an open thalamo-cortico-striatal path, with bidirectional thalamo-insula connections in Model 5. Finally, Model 7 uses a nonlinear DCM to hypothesize the insula as a key influence on the thalamus-to-NAc connection. All interregional connections were allowed to be modulated by DCM-specific regressors of interest—all gain cues, or all loss cues. Like the GLM analysis, the DCM regressors were created using cue-onset times, in order to extend the GLM findings, as well as the findings of previous MID studies that have used cue-onset times (Bjork et al., 2004, 2010; Knutson et al., 2001; Samanez-Larkin et al., 2007).

Region of interest (ROI) extraction

Anatomic masks of the NAc, anterior insula and anteromedial thalamus were searched to determine peak voxels ($p<0.05$, family-wise error [FWE], small-volume corrected) for the contrast all cues vs the neutral cue. Masks for the NAc and insula were hand-drawn masks used in previous studies (Guyer et al., 2006), and for the anteromedial thalamus was an 8 mm sphere approximating this subdivision of the thalamus, based on coordinates from a functional-anatomical map of the thalamus (Johansen-Berg et al., 2005). This contrast was used because both groups and all ROIs showed significant BOLD activations for both the contrasts of all gain-cues vs. neutral cue, and all loss-cues vs. neutral cue, and these peak coordinates were within a few millimeters of each other. For each subject, the principal eigenvariate of all voxels within a 6 mm sphere centered at the associated peak group coordinate ($p<0.05$, FWE, small-volume corrected) were then extracted for each region (see Fig. 4 for a full list of coordinates). In addition, the location of these regions was restricted to subregions with anatomic connections delineated by non-human primate tract-tracing

studies. Coordinates for the insula were restricted to the anterior, agranular division, which projects to the NAc, and is interconnected with the medial thalamus (Chikama et al., 1997; Mufson and Mesulam, 1984). Thalamic coordinates were restricted to the medial aspect of the thalamus in order to target the mediodorsal, midline and intralaminar nuclei, which are limbic subregions interconnected with the NAc and anterior insula (Chikama et al., 1997; Haber et al., 1990; Johansen-Berg et al., 2005; Mufson and Mesulam, 1984; Zhang et al., 2008). All ROI extractions were from the right side of the brain because of the stronger BOLD activation pattern on this side of the brain.

Following ROI extraction, the seven DCM models described above were estimated for each subject. These estimated models underwent Bayesian Model Selection (BMS) in DCM8 to determine the relative best-fit model for each group. The adolescent and adult groups were kept separate during voxel extraction, model selection, and parameter extraction (see below) because of our *a priori* interest in understanding the groups separately.

Bayesian model selection (BMS)

All seven models were tested at the same time, and BMS was done for each group individually. This analysis derives an exceedance probability (ϕ_k, reported here), i.e., the probability that one model is more likely than any other model, given the group data (Stephan et al., 2009, 2010). Note that the exceedance probabilities of all tested models sum to one, and thus the fit of a model to a population is always considered relative to other tested models.

Following selection of the optimal model (highest exceedance probability), the maximum a posteriori (MAP) estimates of each parameter of the best-fit model were extracted for each subject, averaged across runs, and then entered into a random-effects analysis with one-sample t-tests for each group using SPSS (SPSS, Chicago, IL) (Stephan et al., 2010). We assumed no effect of run, and verified this with paired t-tests. Two types of parameters were extracted and reported: 1. the inter-regional connectivity specific to the experiment and irrespective of task effect (termed endogenous connectivity); 2. the modulation of inter-regional connectivity in response to experimental task manipulation, i.e., loss and gain conditions separately.

Parameter weights for anticipation of all gain cues and all loss cues were then entered into a linear mixed model using restricted maximum likelihood estimates for between-group tests. Group, valence (all gain or all loss), and connection (thalamus-to-NAc, thalamus-to-insula, etc.) were entered as fixed factors, using IQ as a covariate of nuisance. Post-hoc tests were corrected using a Bonferroni correction for multiple comparisons.

Results

Behavioral data

Task performance—Three-way ANOVAs of group by valence by magnitude revealed no significant 3-way or 2-way interactions for accuracy (number of successful hits) or reaction time ($p>0.05$). For both accuracy and reaction time, the associated main effects were not significant ($p>0.05$).

Post-scan affective ratings of cues—The three-way ANOVA of group by valence by magnitude was not significant ($p>0.05$). The 2-way valence by magnitude interaction was significant, ($F(2,86)=68.6$, $p<0.001$, $d=1.79$), and there was a significant effect of magnitude among both the loss and gain cues (loss: $F(2,134)=8.1$, $p<0.001$, $d=.49$; gain: $F(2, 135)=7.5$, $p<0.001$, $d=.47$). No other two-way interactions were significant, and the main effect of group was not significant ($p>0.05$). Participants rated loss cues significantly more negatively than gain cues ($p<0.05$, Bonferroni corrected), and the ratings tracked the magnitude of cues ($p<0.05$, Bonferroni corrected). These post-scan affective ratings of cues suggest that both groups accurately learned the relevance of the individual cues, and were similarly aroused. See Fig. 5 for graphical representation.

fMRI data

GLM analyses of local activations—For completeness and validation of the task, and to detail the selection of our ROIs, we first present the GLM analysis of local activations. DCM analysis, the focus of this paper, follows after. We report the small-volume corrected peak activations in the regions commonly activated in the previous studies of the MID task (Bjork and Hommer, 2007; Bjork et al., 2004, 2008, 2010, 2011; Guyer et al., 2006; Knutson et al., 2001; Samanez-Larkin et al., 2007) (Tables 1A,1B). Each group demonstrated a pattern of regional activation including ventral striatum, thalamus, insula, caudate and putamen, similar to that reported in previous publications of the task (Bjork et al., 2004, 2010; Knutson et al., 2001).

All gain cues vs. neutral cue

Adults—Anticipation of all potential monetary gain cues versus the neutral cue was associated with significant activations in NAc (bilateral), caudate (bilateral), putamen (bilateral), thalamus (bilateral), insula (bilateral), and anterior cingulate cortex (bilateral), small-volume corrected (SVC), $p<0.05$, FWE-corrected. See Table 1A.

Adolescents—In adolescents, significant increases in BOLD activity to all gain cues versus the neutral cue were found in regions similar to those seen in adults. These regions included NAc (bilateral), caudate (bilateral), putamen (bilateral), thalamus (right), and insula (bilateral), SVC, $p<0.05$, FWE-corrected. See Table 1A.

Between-group—The putamen (right) and motor cortex (left) were significantly more activated in adults than adolescents, SVC, $p<0.05$, FWE-corrected. No regions were significantly more activated in adolescents than adults, SVC, $p<0.05$, FWE-corrected. See Table 1B.

All loss cues vs. neutral cue

Adults—Anticipation of all loss cues, compared to the neutral cue, was associated with significant activation in NAc (bilateral), caudate (bilateral), putamen (bilateral), insula (right), and thalamus (bilateral), SVC, $p<0.05$, FWE-corrected. See Table 2A for all activated regions.

Adolescents—Anticipation elicited by all loss cues, compared to the neutral cue, led to significant activation in the NAc (bilateral), caudate (left) and thalamus (bilateral), SVC, $p<0.05$, FWE-corrected. See Table 2A for all activated regions.

Between-group—Adults showed significantly higher BOLD signal activation than adolescents in the right putamen, SVC, $p<0.05$, FWE-corrected. For this same contrast, no regions demonstrated significantly more BOLD signal activation in adolescents than adults, SVC, $p<0.05$, FWE-corrected. See Table 2B for all differentially activated regions, SVC, $p<0.05$, FWE-corrected.

All cues vs. neutral cue

This contrast was examined to select coordinates for extracting voxels of interest for DCM.

Adults—In response to anticipation elicited by all cues versus the neutral cue, adults showed significant activation of the NAc (bilateral), caudate (bilateral), putamen (bilateral), thalamus (bilateral), insula (bilateral), and anterior cingulate cortex (bilateral), SVC, $p<0.05$, FWE-corrected. See Table 3A for all activated regions and coordinates.

Adolescents—Adolescents demonstrated significant activation of the NAc (bilateral), caudate (bilateral), putamen (bilateral), and insula (bilateral), SVC, $p<0.05$, FWE-corrected. See Table 3A for all activated regions and coordinates.

Between-group—In response to anticipation of all cues versus the neutral cue, adults showed significantly more activation than adolescents in the putamen (right), SVC, $p<0.05$, FWE-corrected. For this same contrast, adolescents demonstrated significantly more activation in the anterior cingulate cortex (left), SVC, $p<0.05$, FWE-corrected. See Table 3B for all differentially activated regions and coordinates at SVC, $p<0.05$, FWE-corrected.

DCM analysis

Bayesian model selection—A set of seven hypothesized models composed of the NAc, insula and thalamus (see Methods section) were entered into Bayesian Model Selection to determine a best-fit model. Two similarly best-fitting models, Models 1 and 2 (see Figs. 3, 6), emerged for each group. Model 3 followed closely these two models.

See Table 4 and Fig. 6 for exceedance probabilities for adults and adolescents. Models 1 and 2 differed only by one connection. Model 1 was retained for further analysis because it was the most comprehensive one with the fewest a priori constraints.

Model parameter weight extraction

Endogenous connectivity across the whole task is reported first, followed by modulation of this endogenous connectivity by specific task conditions—gain or loss anticipation. See Tables 5-7 for a full list of connectivity weights.

Endogenous connectivity—The sets of endogenous connections with significant connection strengths were similar in the adult group and adolescent group. Both groups

demonstrated significant effective connectivity across the task for the thalamus-to-NAc, thalamus-to-insula, and insula-to-NAc links. The only difference was that adolescents additionally showed significant NAc-to-thalamus connectivity. Parameters for endogenous connectivity can be found in Fig. 7 and Table 5.

Connections modulated by cue class—A schematic of all connections significantly modulated by cue valence ($p<0.05$) is shown in Fig. 8, and Table 6 for adults and Table 7 for adolescents.

Connections modulated by all gain cues

Gain cues significantly modulated only one connection in each group.

Adults (Table 6)—In the adult group, the connection from thalamus-to-NAc was significantly modulated by anticipation of monetary gain cues. There was a trend for the modulation of the thalamus-to-insula connection by gain cues.

Adolescents (Table 7)—In contrast to the adult group, the adolescent group demonstrated significant modulation of the thalamus-to-insula connection by gain cues.

Connections modulated by all loss cues

A number of connections in the incentive processing network were significantly modulated by loss anticipation in both groups.

Adults (Table 6)—Anticipation elicited by loss cues significantly modulated the connectivity of thalamus-to-NAc, insula-to-NAc, and thalamus-to-insula connections in the adult group.

Adolescents (Table 7)—Like the adults, the adolescent group showed significant modulation by loss cues of the thalamus-to-NAc and insula-to-NAc connections. In contrast to the adult group, adolescents showed significant modulation of the insula-to-thalamus and NAc-to-thalamus connections, but not thalamus-to-insula.

Between group comparisons

For the endogenous connectivity, the two-way interaction of group*connection was not significant, and the associated main effects were also not significant, $p>0.05$.

Parameter weights reflecting connectivity modulation by all gain or all loss cues were entered in a linear mixed model. Neither the 3-way interaction of group*valence*connection nor the associated 2-way interactions were significant ($p>0.05$). The main effects of valence and group were not significant ($p>0.05$), however, the main effect of connection was significant, $F(4, 349)=10.7$, $p<0.001$. Pairwise comparisons showed that the modulation of the thalamus-to-NAc and thalamus-to-insula connections were significantly stronger than the modulation of the NAc-to-thalamus, insula-to-NAc, or insula-to-thalamus connections ($p<0.001$, Bonferonni corrected).

Discussion

This study used DCM to examine effective connectivity among the NAc, thalamus, and insula during cue-elicited incentive anticipation in typical adults and adolescents. The DCM analysis yielded three main findings: 1. The best-fit model, independently for both groups, involved all existing anatomic connections, and demonstrated thalamic and insula influences on the NAc. In particular, the thalamus-to-NAc connection was the strongest link of the model. This is the first time that this directional link has been demonstrated in humans in the context of reward processing; 2. In contrast to expectation, the number of significant connections was higher in the loss-cue condition than the gain-cue condition in both groups; 3. Finally, contrary to our predictions, between-group comparisons of connectivity strength failed to detect statistical differences. In general, task-elicited BOLD activations were similar to previous studies of this paradigm in adults and adolescents (Bjork et al., 2004, 2010; Knutson et al., 2001). Also, in line with previous work (Bjork et al., 2004, 2010), adults activated the striatum more strongly than did adolescents. Findings in the current study emerged in a different striatal region, here putamen and in previous work, NAc extending into dorsal striatum. Nevertheless, in all three studies, the MID task elicited robust activation of both the adult and adolescent striatum, with *relative* hypoactivation of the striatum in adolescents, compared with adults. These results are presented for completeness, but their discussion is beyond the scope of this paper.

Functional circuitry of incentive processing—endogenous connectivity

The best-fit model of incentive processing included functional connections among all regions with established anatomic connections. Additionally, this best-fit model was the same for each group, demonstrating replication in two independent samples. Examination of the significant endogenous connectivity revealed a core incentive processing network involving the NAc, thalamus and insula (Fig. 7). Adults and adolescents recruited networks with similar endogenous connectivity, and both groups demonstrated thalamic influence on insula and NAc, as well as insula influence on the NAc. Adolescents additionally demonstrated significant connectivity of the NAc-to-thalamus connection, though the strength of this connection did not significantly differ from that in adults, for whom no evidence of NAc-to-thalamus connectivity emerged. While the NAc has long been associated with incentive processing (Breiter and Rosen, 1999; Colle and Wise, 1988; Delgado et al., 2000; Ikemoto et al., 1997; Knutson et al., 2001), the current study highlights the thalamus and insula as important functional influences on the NAc during incentive processing.

Traditionally described as a relay system, the thalamus also participates in associative processes, as demonstrated by animal studies examining discriminative approach and avoidance learning, context-induced reward seeking, and anticipation of unpleasant stimuli (Chandrasekhar et al., 2008; Freeman et al., 1996; Groenewegen and Berendse, 1994; Hamlin et al., 2009; Herwig et al., 2007; Smith et al., 2002; Van der Werf et al., 2002). Like the thalamus, the anterior insula is often reported in fMRI studies as showing increased BOLD activation during incentive processing (Chandrasekhar et al., 2008; Herwig et al., 2007; Knutson and Greer, 2008; Liu et al., 2011; Paulus et al., 2003; Villafuerte et al.,

2011). In contrast to the thalamus, however, the insula is a cortical site for highly processed interoceptive and exteroceptive, information, and here may code for the somatic/autonomic changes that occur in response to incentive exposure (Craig, 2003, 2004; Naqvi et al., 2007; Villafuerte et al., 2011). In addition, BOLD activations of the insula and NAc have recently been found to be associated with individual variations in motivation (Clithero et al., 2011). In our study, the significant endogenous connectivity of the thalamus-to-insula-to-NAc path, and thalamus-to-NAc path in both adolescents and adults suggests that the insula and thalamus may provide the NAc with information about drive (from interoceptive signals) and opportunity (from exteroceptive signals), respectively, for incentive processing.

Cue-elicited reward and loss anticipation

The modulation of the endogenous connectivity by cue-elicited gain or loss anticipation was separately examined. In both adolescents and adults, loss anticipation modulated the incentive-processing network more broadly than gain anticipation, and loss specifically modulated connections involving the insula with the NAc.

Cue-elicited gain anticipation modulated the thalamus-to-NAc connection in adults, and thalamus-to-insula connection in adolescents. These patterns reflected within-group variations only, and the groups were not found to directly differ on statistical grounds. In adults, the prominence of the thalamus-to-NAc connectivity (Fig. 8) contrasts with the direction of the striato-thalamo-cortico-striatal loops. This finding may reflect the early phase of reward processing that was modeled in this study (recognition of motivational cues) and the substantial glutamatergic projection from the thalamus to the NAc (Christie et al., 1987; Gimenez-Amaya et al., 1995). The significant modulation of the thalamus-to-NAc connectivity also supports the hypothesis that the thalamus gates striatal activity to modulate attentional or motor responses, and cortical input (Groenewegen and Berendse, 1994; Haber and McFarland, 2001). Similarly, animal studies have demonstrated increased dopamine efflux in the NAc following medial thalamus stimulation, and functionally, this path has been shown to contribute to the renewal of context-induced reward seeking (Hamlin et al., 2009; Parsons et al., 2007; Pinto et al., 2003). The present study provides evidence for the importance of the thalamus-NAc pathway in human adults during reward processing, specifically during cue-elicited reward anticipation. Because of the lack of statistical group differences in the connectivity strengths, it would be inappropriate to discuss the distinct patterns of connectivity apparent on inspection of Fig. 8.

Cue-elicited loss anticipation seemed to modulate a broader set of connections than gain anticipation (Fig. 8), though the modulation strength was not significantly different between both conditions. Interestingly, in this study, cue-elicited loss anticipation modulated connections involving the insula to NAc (Fig. 8). Insula activation, particularly in the right hemisphere, has been reported in response to a wide variety of negatively-valenced stimuli, findings related to its proposed role in interoception. Insula activation has been shown in response to faces expressing disgust (Phillips et al., 1997), under risk-aversive conditions, (Liu et al., 2007; Paulus et al., 2003; Xue et al., 2010), and during anticipation or presentation of aversive visual stimuli or pain (Mataix-Cols et al., 2008; Wiech et al., 2010). In our study and others, insula and NAc BOLD activation occurred during both reward and

loss anticipation (Bjork et al., 2004, 2010; Knutson et al., 2001; Samanez-Larkin et al., 2007), and DCM revealed that only cue-elicited loss anticipation strengthened significantly the insula-to-NAc connectivity in both groups. The insula's influence on the NAc may help discriminate negatively-valenced stimuli and, thus, facilitate appropriate behavioral responses from the NAc.

Finally, though this study did not show a significant effect of valence among the connections, a significant effect of connection was found. Specifically, the thalamus-to-NAc and thalamus-to-insula connectivity were found to be significantly stronger than other connections across both groups. Thus, the thalamus appeared to be a central node in both cue-elicited gain and loss anticipation. As discussed earlier, this likely reflects its role in processing salient exteroceptive information to redirect attention and behavior, a function that may be achieved through activation of cholinergic interneurons (Ding et al., 2010; Matsumoto et al., 2001; Smith et al., 2011). These results highlight the importance of the thalamus in reward processing, and its influence on key reward regions. As this area of study is not well understood yet, future research should more specifically address the role of thalamic effective connectivity in reward processing.

Developmental comparisons

The third main finding of the present study is the absence of statistically significant differences in connectivity modulation between adolescents and adults. This finding was unexpected, and could reflect high individual variability in effective connectivity measures that might warrant larger sample sizes to detect group differences. The wide age range in each group might also have contributed to an increased variability and, in turn, difficulty detecting group differences. However, restricting age in each group (13–16 years old for the adolescents, and 20–30 years old for the adults) did not change the results, perhaps a reflection of the reduced sample size (data not shown). Additionally, neural regions outside of those included in our study may be responsible for developmental differences.

The non-significance of our between-group findings is difficult to interpret due to the lack of studies on incentive processing connectivity concomitantly in both age groups. This is the first study to use DCM with this task in healthy adolescents and adults. The non-significance of the connectivity strengths between groups are in contrast to findings of group-differences in striatal activation, in the present work as well as in previous fMRI-activation studies (Bjork et al., 2004, 2010; Ernst and Fudge, 2009; Ernst et al., 2005; Galvan, 2010; Galvan et al., 2006; Geier et al., 2010; Spear, 2000; Van Leijenhorst et al., 2010a). Because this is the first study of its kind, it warrants replication, and more research is needed to understand the adolescent-specific associated neural circuitry, and how this informs decision-making across development.

Study limitations

Our model was restricted to a minimal number of nodes and did not include other reward-related regions, such as orbitofrontal cortex, dopaminergic midbrain, medial pre-frontal cortex, amygdala, or globus pallidus (Knutson and Greer, 2008; Liu et al., 2011; O'Doherty, 2004). These regions, while important, were not consistently activated in this study (or other

MID studies), a requirement for DCM. The number of nodes was also purposely limited to avoid model over-fitting and to increase generalizability.

In addition, only connectivity associated with regions of the right side of the brain were examined, because of its stronger activation patterns. Although the subject of debate, laterality may have been affected by the task. Further work is needed to test this possibility. Future work may also examine finer age discriminations. Finally, we did not test sex effects because of the lack of *a priori* hypotheses.

Conclusions and future directions

This study used DCM and the MID task to provide evidence for a core incentive processing network involving the NAc, thalamus and anterior insula in typical adults and adolescents. Both groups demonstrated similar endogenous connectivity of the core incentive processing network, and demonstrated thalamic and insula influences on the NAc, suggesting that these regions may provide the NAc with exteroceptive signals about cues and interoceptive signals about drive. In addition, in both groups, cue-elicited loss anticipation modulated the connections involving the insula to the NAc. This is the first study of effective connectivity of the MID task in both adults and adolescents. This study also provides novel information regarding the role of the thalamus in reward anticipation. Taken together, considering the novelty of these findings, replication is warranted before drawing further conclusions. Finally, future studies may involve testing this incentive-processing network across different tasks or reward phases, a larger model space, or younger or older age groups.

Acknowledgments

We wish to acknowledge Professor Joy Geng for her help on DCM methods.

References

Alexander WH, Brown JW. Competition between learned reward and error outcome predictions in anterior cingulate cortex. Neuroimage. 2010; 49:3210–3218. [PubMed: 19961940]

Asato MR, Terwilliger R, Woo J, Luna B. White matter development in adolescence: a DTI study. Cereb. Cortex. 2010; 20:2122–2131. [PubMed: 20051363]

Barnea-Goraly N, Menon V, Eckert M, Tamm L, Bammer R, Karchemskiy A, Dant CC, Reiss AL. White matter development during childhood and adolescence: a cross-sectional diffusion tensor imaging study. Cereb. Cortex. 2005; 15:1848–1854. [PubMed: 15758200]

Bjork JM, Hommer DW. Anticipating instrumentally obtained and passively-received rewards: a factorial fMRI investigation. Behav. Brain Res. 2007; 177:165–170. [PubMed: 17140674]

Bjork JM, Knutson B, Fong GW, Caggiano DM, Bennett SM, Hommer DW. Incentive-elicited brain activation in adolescents: similarities and differences from young adults. J. Neurosci. 2004; 24:1793–1802. [PubMed: 14985419]

Bjork JM, Smith AR, Hommer DW. Striatal sensitivity to reward deliveries and omissions in substance dependent patients. Neuroimage. 2008; 42:1609–1621. [PubMed: 18672069]

Bjork JM, Smith AR, Chen G, Hommer DW. Adolescents, adults and rewards: comparing motivational neurocircuitry recruitment using fMRI. PLoS One. 2010; 5:e11440. [PubMed: 20625430]

Bjork JM, Smith AR, Chen G, Hommer DW. Mesolimbic recruitment by nondrug rewards in detoxified alcoholics: effort anticipation, reward anticipation, and reward delivery. Hum. Brain Mapp. 2012; 33:2174–2188. [PubMed: 22281932]

Breiter HC, Rosen BR. Functional magnetic resonance imaging of brain reward circuitry in the human. Ann. N. Y. Acad. Sci. 1999; 877:523–547. [PubMed: 10415669]

Breiter HC, Aharon I, Kahneman D, Dale A, Shizgal P. Functional imaging of neural responses to expectancy and experience of monetary gains and losses. Neuron. 2001; 30:619–639. [PubMed: 11395019]

Cauda F, Cavanna AE, D'Agata F, Sacco K, Duca S, Geminiani GC. Functional connectivity and coactivation of the nucleus accumbens: a combined functional connectivity and structure-based meta-analysis. J. Cogn. Neurosci. 2011; 23:2864–2877. [PubMed: 21265603]

Chandrasekhar PV, Capra CM, Moore S, Noussair C, Berns GS. Neurobiological regret and rejoice functions for aversive outcomes. Neuroimage. 2008; 39:1472–1484. [PubMed: 18042401]

Chikama M, McFarland NR, Amaral DG, Haber SN. Insular cortical projections to functional regions of the striatum correlate with cortical cytoarchitectonic organization in the primate. J. Neurosci. 1997; 17:9686–9705. [PubMed: 9391023]

Christakou A, Brammer M, Rubia K. Maturation of limbic corticostriatal activation and connectivity associated with developmental changes in temporal discounting. Neuroimage. 2011; 54:1344–1354. [PubMed: 20816974]

Christie MJ, Summers RJ, Stephenson JA, Cook CJ, Beart PM. Excitatory amino acid projections to the nucleus accumbens septi in the rat: a retrograde transport study utilizing D[^{3}H]aspartate and [^{3}H]GABA. Neuroscience. 1987; 22:425–439. [PubMed: 2823173]

Clark L, Bechara A, Damasio H, Aitken MR, Sahakian BJ, Robbins TW. Differential effects of insular and ventromedial prefrontal cortex lesions on risky decision-making. Brain. 2008; 131:1311–1322. [PubMed: 18390562]

Clithero JA, Reeck C, Carter RM, Smith DV, Huettel SA. Nucleus accumbens mediates relative motivation for rewards in the absence of choice. Front. Hum. Neurosci. 2011; 5:87. [PubMed: 21941472]

Cohen JR, Asarnow RF, Sabb FW, Bilder RM, Bookheimer SY, Knowlton BJ, Poldrack RA. A unique adolescent response to reward prediction errors. Nat. Neurosci. 2010; 13:669–671. [PubMed: 20473290]

Colle LM, Wise RA. Effects of nucleus accumbens amphetamine on lateral hypothalamic brain stimulation reward. Brain Res. 1988; 459:361–368. [PubMed: 3179710]

Cooper JC, Knutson B. Valence and salience contribute to nucleus accumbens activation. Neuroimage. 2008; 39:538–547. [PubMed: 17904386]

Craig AD. How do you feel? Interoception: the sense of the physiological condition of the body. Nat. Rev. Neurosci. 2002; 3:655–666. [PubMed: 12154366]

Craig AD. Interoception: the sense of the physiological condition of the body. Curr. Opin. Neurobiol. 2003; 13:500–505. [PubMed: 12965300]

Craig AD. Human feelings: why are some more aware than others? Trends Cogn. Sci. 2004; 8:239–241. [PubMed: 15165543]

Craig AD. How do you feel—now? The anterior insula and human awareness. Nat. Rev. Neurosci. 2009; 10:59–70. [PubMed: 19096369]

Damasio AR. The Feeling of What Happens: Body and Emotion in the Making of Consciousness: Mariner Books. 1999

Delgado MR, Nystrom LE, Fissell C, Noll DC, Fiez JA. Tracking the hemodynamic responses to reward and punishment in the striatum. J. Neurophysiol. 2000; 84:3072–3077. [PubMed: 11110834]

Ding JB, Guzman JN, Peterson JD, Goldberg JA, Surmeier DJ. Thalamic gating of corticostriatal signaling by cholinergic interneurons. Neuron. 2010; 67:294–307. [PubMed: 20670836]

Duncan J, Owen AM. Common regions of the human frontal lobe recruited by diverse cognitive demands. Trends Neurosci. 2000; 23:475–483. [PubMed: 11006464]

Ernst M, Fudge JL. A developmental neurobiological model of motivated behavior: anatomy, connectivity and ontogeny of the triadic nodes. Neurosci. Biobehav. Rev. 2009; 33:367–382. [PubMed: 19028521]

Ernst M, Nelson EE, Jazbec S, McClure EB, Monk CS, Leibenluft E, Blair J, Pine DS. Amygdala and nucleus accumbens in responses to receipt and omission of gains in adults and adolescents. Neuroimage. 2005; 25:1279–1291. [PubMed: 15850746]

Fair DA, Cohen AL, Dosenbach NU, Church JA, Miezin FM, Barch DM, Raichle ME, Petersen SE, Schlaggar BL. The maturing architecture of the brain's default network. Proc. Natl. Acad. Sci. U.S.A. 2008; 105:4028–4032. [PubMed: 18322013]

Freeman JH Jr. Cuppernell C, Flannery K, Gabriel M. Context-specific multisite cingulate cortical, limbic thalamic, and hippocampal neuronal activity during concurrent discriminative approach and avoidance training in rabbits. J. Neurosci. 1996; 16:1538–1549. [PubMed: 8778303]

Friston KJ, Harrison L, Penny W. Dynamic causal modelling. Neuroimage. 2003; 19:1273–1302. [PubMed: 12948688]

Galvan A. Adolescent development of the reward system. Front. Hum. Neurosci. 2010; 4:6. [PubMed: 20179786]

Galvan A, Hare TA, Parra CE, Penn J, Voss H, Glover G, Casey BJ. Earlier development of the accumbens relative to orbitofrontal cortex might underlie risk-taking behavior in adolescents. J. Neurosci. 2006; 26:6885–6892. [PubMed: 16793895]

Geier CF, Terwilliger R, Teslovich T, Velanova K, Luna B. Immaturities in reward processing and its influence on inhibitory control in adolescence. Cereb. Cortex. 2010; 20:1613–1629. [PubMed: 19875675]

Gilbert SJ, Henson RN, Simons JS. The scale of functional specialization within human prefrontal cortex. J. Neurosci. 2010; 30:1233–1237. [PubMed: 20107051]

Gimenez-Amaya JM, McFarland NR, de las Heras S, Haber SN. Organization of thalamic projections to the ventral striatum in the primate. J. Comp. Neurol. 1995; 354:127–149. [PubMed: 7542290]

Gonen T, Admon R, Podlipsky I, Hendler T. From animal model to human brain networking: dynamic causal modeling of motivational systems. J. Neurosci. 2012; 32:7218–7224. [PubMed: 22623666]

Groenewegen HJ, Berendse HW. The specificity of the 'nonspecific' midline and intralaminar thalamic nuclei. Trends Neurosci. 1994; 17:52–57. [PubMed: 7512768]

Group, B.D.C. Total and regional brain volumes in a population-based normative sample from 4 to 18 years: the NIH MRI Study of Normal Brain Development. Cereb. Cortex. 2012; 22:1–12. [PubMed: 21613470]

Gu H, Salmeron BJ, Ross TJ, Geng X, Zhan W, Stein EA, Yang Y. Mesocorticolimbic circuits are impaired in chronic cocaine users as demonstrated by resting-state functional connectivity. Neuroimage. 2010; 53:593–601. [PubMed: 20603217]

Guyer AE, Nelson EE, Perez-Edgar K, Hardin MG, Roberson-Nay R, Monk CS, Bjork JM, Henderson HA, Pine DS, Fox NA, Ernst M. Striatal functional alteration in adolescents characterized by early childhood behavioral inhibition. J. Neurosci. 2006; 26:6399–6405. [PubMed: 16775126]

Haber SN. The primate basal ganglia: parallel and integrative networks. J. Chem. Neuroanat. 2003; 26:317–330. [PubMed: 14729134]

Haber SN, Knutson B. The reward circuit: linking primate anatomy and human imaging. Neuropsychopharmacology. 2010; 35:4–26. [PubMed: 19812543]

Haber S, McFarland NR. The place of the thalamus in frontal cortical-basal ganglia circuits. Neuroscientist. 2001; 7:315–324. [PubMed: 11488397]

Haber SN, Lynd E, Klein C, Groenewegen HJ. Topographic organization of the ventral striatal efferent projections in the rhesus monkey: an anterograde tracing study. J. Comp. Neurol. 1990; 293:282–298. [PubMed: 19189717]

Hamlin AS, Clemens KJ, Choi EA, McNally GP. Paraventricular thalamus mediates context-induced reinstatement (renewal) of extinguished reward seeking. Eur. J. Neurosci. 2009; 29:802–812. [PubMed: 19200064]

Hardin MG, Ernst M. Functional brain imaging of development-related risk and vulnerability for substance use in adolescents. J. Addic.t Med. 2009; 3:47–54.

Hasan KM, Walimuni IS, Abid H, Frye RE, Ewing-Cobbs L, Wolinsky JS, Narayana PA. Multimodal quantitative magnetic resonance imaging of thalamic development and aging across the human lifespan: implications to neurodegeneration in multiple sclerosis. J. Neurosci. 2011; 31:16826–16832. [PubMed: 22090508]

Herwig U, Baumgartner T, Kaffenberger T, Bruhl A, Kottlow M, Schreiter-Gasser U, Abler B, Jancke L, Rufer M. Modulation of anticipatory emotion and perception processing by cognitive control. Neuroimage. 2007; 37:652–662. [PubMed: 17588776]

Ikemoto S, Glazier BS, Murphy JM, McBride WJ. Role of dopamine D1 and D2 receptors in the nucleus accumbens in mediating reward. J. Neurosci. 1997; 17:8580–8587. [PubMed: 9334429]

Jensen J, McIntosh AR, Crawley AP, Mikulis DJ, Remington G, Kapur S. Direct activation of the ventral striatum in anticipation of aversive stimuli. Neuron. 2003; 40:1251–1257. [PubMed: 14687557]

Jia Z, Worhunsky PD, Carroll KM, Rounsaville BJ, Stevens MC, Pearlson GD, Potenza MN. An initial study of neural responses to monetary incentives as related to treatment outcome in cocaine dependence. Biol. Psychiatry. 2011; 70:553–560. [PubMed: 21704307]

Johansen-Berg H, Behrens TE, Sillery E, Ciccarelli O, Thompson AJ, Smith SM, Matthews PM. Functional–anatomical validation and individual variation of diffusion tractography-based segmentation of the human thalamus. Cereb. Cortex. 2005; 15:31–39. [PubMed: 15238447]

Kaufman J, Birmaher B, Brent D, Rao U, Flynn C, Moreci P, Williamson D, Ryan N. Schedule for Affective Disorders and Schizophrenia for School-Age Children-Present and Lifetime Version (K-SADS-PL): initial reliability and validity data. J. Am. Acad. Child Adolesc. Psychiatry. 1997; 36:980–988. [PubMed: 9204677]

Kelly AM, Di Martino A, Uddin LQ, Shehzad Z, Gee DG, Reiss PT, Margulies DS, Castellanos FX, Milham MP. Development of anterior cingulate functional connectivity from late childhood to early adulthood. Cereb. Cortex. 2009; 19:640–657. [PubMed: 18653667]

Knutson B, Greer SM. Anticipatory affect: neural correlates and consequences for choice. Philos. Trans. R. Soc. Lond. B Biol. Sci. 2008; 363:3771–3786. [PubMed: 18829428]

Knutson B, Adams CM, Fong GW, Hommer D. Anticipation of increasing monetary reward selectively recruits nucleus accumbens. J. Neurosci. 2001; 21:RC159. [PubMed: 11459880]

Liu X, Powell DK, Wang H, Gold BT, Corbly CR, Joseph JE. Functional dissociation in frontal and striatal areas for processing of positive and negative reward information. J. Neurosci. 2007; 27:4587–4597. [PubMed: 17460071]

Liu X, Hairston J, Schrier M, Fan J. Common and distinct networks underlying reward valence and processing stages: a meta-analysis of functional neuroimaging studies. Neurosci. Biobehav. Rev. 2011; 35:1219–1236. [PubMed: 21185861]

Mataix-Cols D, An SK, Lawrence NS, Caseras X, Speckens A, Giampietro V, Brammer MJ, Phillips ML. Individual differences in disgust sensitivity modulate neural responses to aversive/disgusting stimuli. Eur. J. Neurosci. 2008; 27:3050–3058. [PubMed: 18588543]

Matsumoto N, Minamimoto T, Graybiel AM, Kimura M. Neurons in the thalamic CM-Pf complex supply striatal neurons with information about behaviorally significant sensory events. J. Neurophysiol. 2001; 85:960–976. [PubMed: 11160526]

Mogenson GJ, Jones DL, Yim CY. From motivation to action: functional interface between the limbic system and the motor system. Prog. Neurobiol. 1980; 14:69–97. [PubMed: 6999537]

Mufson EJ, Mesulam MM. Thalamic connections of the insula in the rhesus monkey and comments on the paralimbic connectivity of the medial pulvinar nucleus. J. Comp. Neurol. 1984; 227:109–120. [PubMed: 6470205]

Mufson EJ, Mesulam MM, Pandya DN. Insular interconnections with the amygdala in the rhesus monkey. Neuroscience. 1981; 6:1231–1248. [PubMed: 6167896]

Naqvi NH, Bechara A. The hidden island of addiction: the insula. Trends Neurosci. 2009; 32:56–67. [PubMed: 18986715]

Naqvi NH, Rudrauf D, Damasio H, Bechara A. Damage to the insula disrupts addiction to cigarette smoking. Science. 2007; 315:531–534. [PubMed: 17255515]

Nieuwenhuys R. The insular cortex: a review. Prog. Brain Res. 2012; 195:123–163. [PubMed: 22230626]

Nishijo H, Ono T, Nishino H. Single neuron responses in amygdala of alert monkey during complex sensory stimulation with affective significance. J. Neurosci. 1988; 8:3570–3583. [PubMed: 3193171]

O'Doherty JP. Reward representations and reward-related learning in the human brain: insights from neuroimaging. Curr. Opin. Neurobiol. 2004; 14:769–776. [PubMed: 15582382]

Parsons MP, Li S, Kirouac GJ. Functional and anatomical connection between the paraventricular nucleus of the thalamus and dopamine fibers of the nucleus accumbens. J. Comp. Neurol. 2007; 500:1050–1063. [PubMed: 17183538]

Paulus MP, Rogalsky C, Simmons A, Feinstein JS, Stein MB. Increased activation in the right insula during risk-taking decision making is related to harm avoidance and neuroticism. Neuroimage. 2003; 19:1439–1448. [PubMed: 12948701]

Phillips ML, Young AW, Senior C, Brammer M, Andrew C, Calder AJ, Bullmore ET, Perrett DI, Rowland D, Williams SC, Gray JA, David AS. A specific neural substrate for perceiving facial expressions of disgust. Nature. 1997; 389:495–498. [PubMed: 9333238]

Pinto A, Jankowski M, Sesack SR. Projections from the paraventricular nucleus of the thalamus to the rat prefrontal cortex and nucleus accumbens shell: ultrastructural characteristics and spatial relationships with dopamine afferents. J. Comp. Neurol. 2003; 459:142–155. [PubMed: 12640666]

Robbins TW, Everitt BJ. Neurobehavioural mechanisms of reward and motivation. Curr. Opin. Neurobiol. 1996; 6:228–236. [PubMed: 8725965]

Roesch MR, Singh T, Brown PL, Mullins SE, Schoenbaum G. Ventral striatal neurons encode the value of the chosen action in rats deciding between differently delayed or sized rewards. J. Neurosci. 2009; 29:13365–13376. [PubMed: 19846724]

Samanez-Larkin GR, Gibbs SE, Khanna K, Nielsen L, Carstensen LL, Knutson B. Anticipation of monetary gain but not loss in healthy older adults. Nat. Neurosci. 2007; 10:787–791. [PubMed: 17468751]

Smith DM, Freeman JH Jr. Nicholson D, Gabriel M. Limbic thalamic lesions, appetitively motivated discrimination learning, and training-induced neuronal activity in rabbits. J. Neurosci. 2002; 22:8212–8221. [PubMed: 12223575]

Smith Y, Surmeier DJ, Redgrave P, Kimura M. Thalamic contributions to basal ganglia-related behavioral switching and reinforcement. J. Neurosci. 2011; 31:16102–16106. [PubMed: 22072662]

Sowell ER, Trauner DA, Gamst A, Jernigan TL. Development of cortical and subcortical brain structures in childhood and adolescence: a structural MRI study. Dev. Med. Child Neurol. 2002; 44:4–16. [PubMed: 11811649]

Spear LP. The adolescent brain and age-related behavioral manifestations. Neurosci. Biobehav. Rev. 2000; 24:417–463. [PubMed: 10817843]

Spitzer RL, Williams JB, Gibbon M, First MB. The Structured Clinical Interview for DSM-III-R (SCID). I: History, rationale, and description. Arch. Gen. Psychiatry. 1992; 49:624–629. [PubMed: 1637252]

Stephan KE, Kasper L, Harrison LM, Daunizeau J, den Ouden HE, Breakspear M, Friston KJ. Nonlinear dynamic causal models for fMRI. Neuroimage. 2008; 42:649–662. [PubMed: 18565765]

Stephan KE, Penny WD, Daunizeau J, Moran RJ, Friston KJ. Bayesian model selection for group studies. Neuroimage. 2009; 46:1004–1017. [PubMed: 19306932]

Stephan KE, Penny WD, Moran RJ, den Ouden HE, Daunizeau J, Friston KJ. Ten simple rules for dynamic causal modeling. Neuroimage. 2010; 49:3099–3109. [PubMed: 19914382]

Stevens MC, Pearlson GD, Calhoun VD. Changes in the interaction of resting-state neural networks from adolescence to adulthood. Hum. Brain Mapp. 2009; 30:2356–2366. [PubMed: 19172655]

Tom SM, Fox CR, Trepel C, Poldrack RA. The neural basis of loss aversion in decision-making under risk. Science. 2007; 315:515–518. [PubMed: 17255512]

Tzourio-Mazoyer N, Landeau B, Papathanassiou D, Crivello F, Etard O, Delcroix N, Mazoyer B, Joliot M. Automated anatomical labeling of activations in SPM using a macroscopic anatomical parcellation of the MNI MRI single-subject brain. Neuroimage. 2002; 15:273–289. [PubMed: 11771995]

Van der Werf YD, Witter MP, Groenewegen HJ. The intralaminar and midline nuclei of the thalamus. Anatomical and functional evidence for participation in processes of arousal and awareness. Brain Res. Brain Res. Rev. 2002; 39:107–140. [PubMed: 12423763]

Van Leijenhorst L, Zanolie K, Van Meel CS, Westenberg PM, Rombouts SA, Crone EA. What motivates the adolescent? Brain regions mediating reward sensitivity across adolescence. Cereb. Cortex. 2010a; 20:61–69. [PubMed: 19406906]

Van Leijenhorst L, Gunther Moor B, Op de Macks ZA, Rombouts SA, Westenberg PM, Crone EA. Adolescent risky decision-making: neurocognitive development of reward and control regions. Neuroimage. 2010b; 51:345–355. [PubMed: 20188198]

Veldhuizen MG, Douglas D, Aschenbrenner K, Gitelman DR, Small DM. The anterior insular cortex represents breaches of taste identity expectation. J. Neurosci. 2011; 31:14735–14744. [PubMed: 21994389]

Villafuerte S, Heitzeg MM, Foley S, Wendy Yau WY, Majczenko K, Zubieta JK, Zucker RA, Burmeister M. Impulsiveness and insula activation during reward anticipation are associated with genetic variants in GABRA2 in a family sample enriched for alcoholism. Mol. Psychiatry. 2012; 17:511–519. [PubMed: 21483437]

Wiech K, Lin CS, Brodersen KH, Bingel U, Ploner M, Tracey I. Anterior insula integrates information about salience into perceptual decisions about pain. J. Neurosci. 2010; 30:16324–16331. [PubMed: 21123578]

Xue G, Lu Z, Levin IP, Bechara A. The impact of prior risk experiences on subsequent risky decision-making: the role of the insula. Neuroimage. 2010; 50:709–716. [PubMed: 20045470]

Zhang D, Snyder AZ, Fox MD, Sansbury MW, Shimony JS, Raichle ME. Intrinsic functional relations between human cerebral cortex and thalamus. J. Neurophysiol. 2008; 100:1740–1748. [PubMed: 18701759]

Zink CF, Pagnoni G, Martin ME, Dhamala M, Berns GS. Human striatal response to salient nonrewarding stimuli. J. Neurosci. 2003; 23:8092–8097. [PubMed: 12954871]

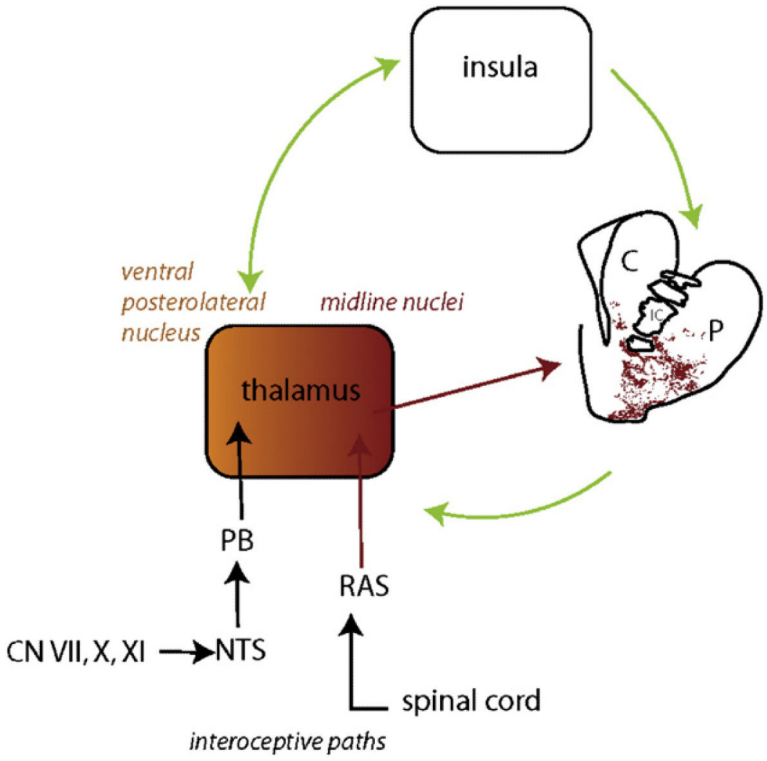

Fig. 1.

Anatomic interconnections among nucleus accumbens (NAc), thalamus and insula. Midline thalamus also gets input from reticular activating system (RAS) and brainstem regions: nucleus tractus solitarius (NTS) and parabrachial (PB) nucleus. There are bidirectional connections between thalamus and insula, and thalamus and NAc (there is a small direct NAc to thalamus projection, as well as a larger indirect connection, through the globus pallidus). There is a unidirectional connection between insula and NAc.

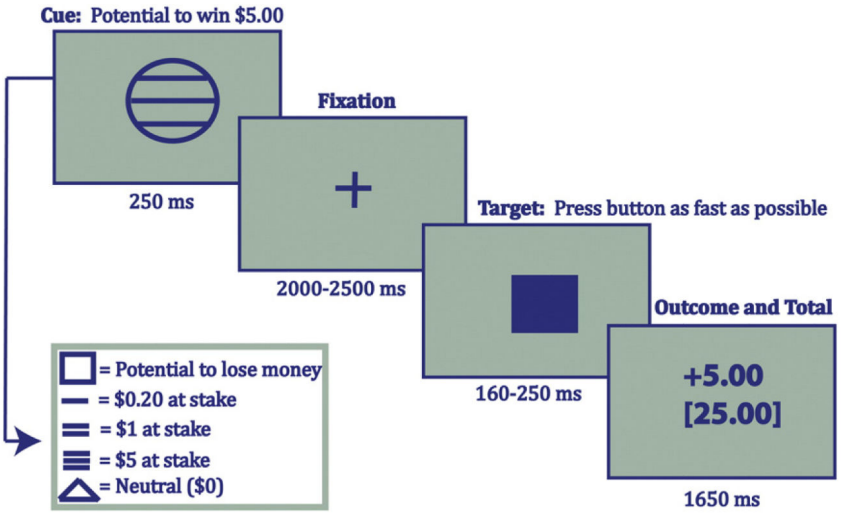

Fig. 2.

Schematic of monetary incentive delay (MID) task. Subjects saw a cue representing the amount of money to be won or lost, followed by fixation, then a target to press the button as fast as possible. The outcome of the trial and total earnings were then presented. Circle cues represented the potential to win money, square cues the potential to lose money, and triangle cues no money (neutral cue). Within the shapes, one line represented $0.20 at stake, two lines $1, and three lines $5. The GLM and DCM analysis used the cue-onset times to model cue-elicited anticipation.

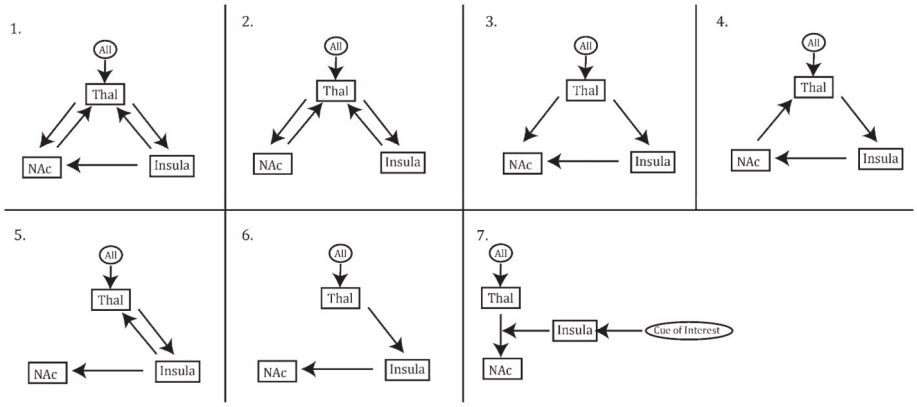

Fig. 3.

The schematic for all seven tested models. All models represent iterations based on the fully-connected, anatomically-relevant model, Model 1, as defined by anatomic connections found in the non-human primate literature. Briefly, Model 2 posits the thalamus as the central processing region, independently communicating with the NAc and insula. Model 3 posits the NAc as the final receiving site of incentive information, and Model 4 demonstrates a closed-loop model based on the striato-thalamo-cortico-striatal loop model. Models 5 and 6 posit an open thalamo-cortico-striatal path, with bidirectional thalamo-insula connections in Model 5. Finally, Model 7, based on a nonlinear DCM, posits the insula as a key influence on the thalamus-to-NAc connection.

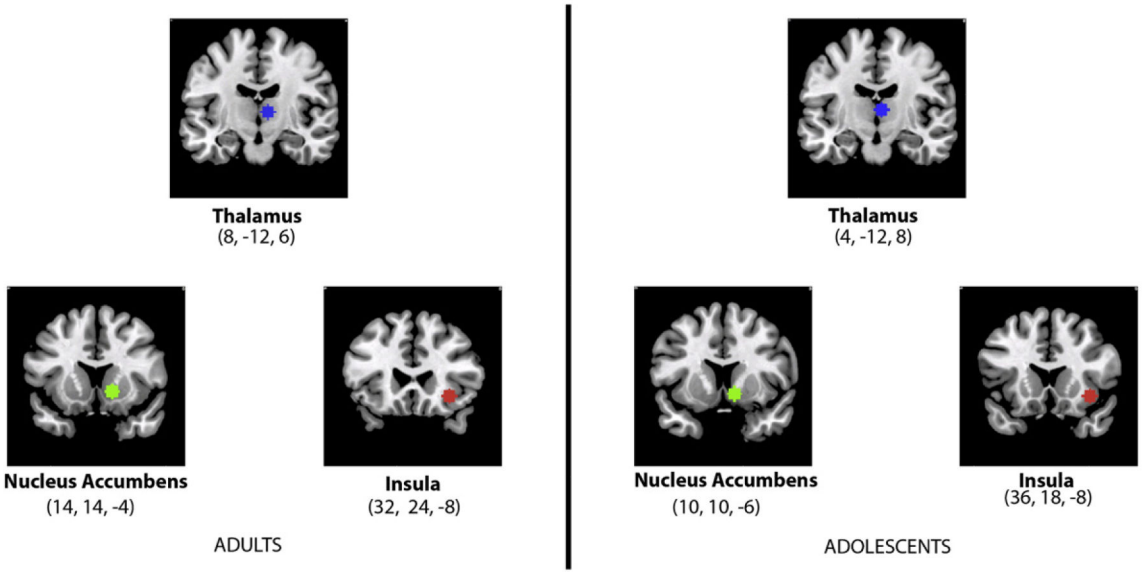

Fig. 4.

Masks for ROI extraction. All voxels within a 6 mm sphere centered on the group peak coordinates for the contrast 'all cues vs. the neutral cue' were extracted for each subject. Coordinates refer to MNI space and represent the group peak coordinates (center of the sphere).

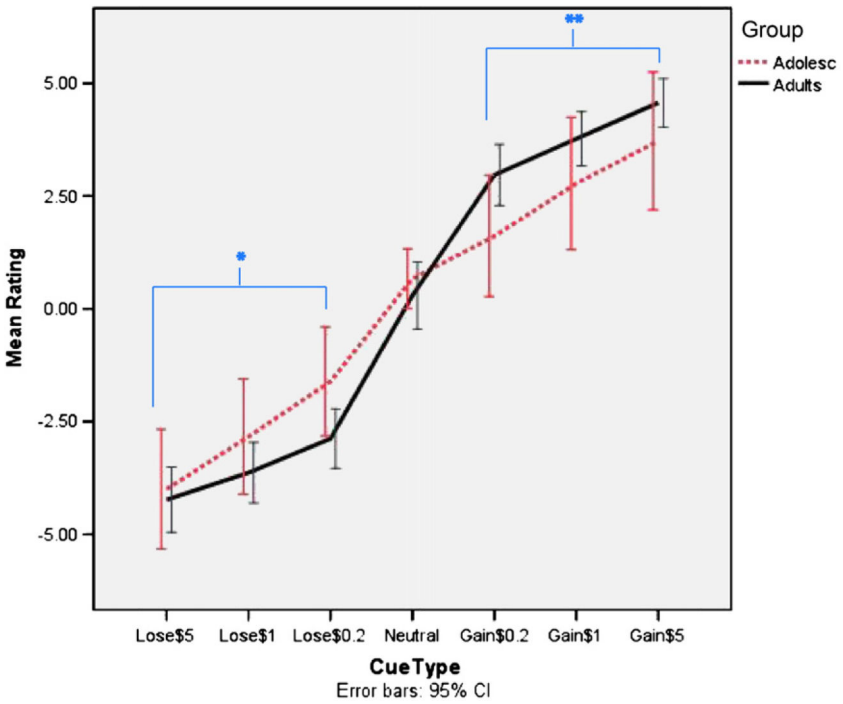

Fig. 5.

Post-scan ratings of cue "liking". Participants rated how much they liked or disliked each cue type after they finished the task. There was a significant interaction between valence and magnitude ($p<0.001$), and there was a significant effect of magnitude among both the loss and gain cues ($p<0.001$ for each). Blue lines represent the significant pairwise comparisons among the cue types. *Participants significantly disliked the Lose $5 cue more than the Lose $0.20 cue, $p<0.001$, Bonf. corrected. **Participants significantly preferred the Gain $5 cue to the Gain $0.20 cue, $p<0.001$, Bonf. corrected. −5 = Dislike very much. +5 = Like very much.

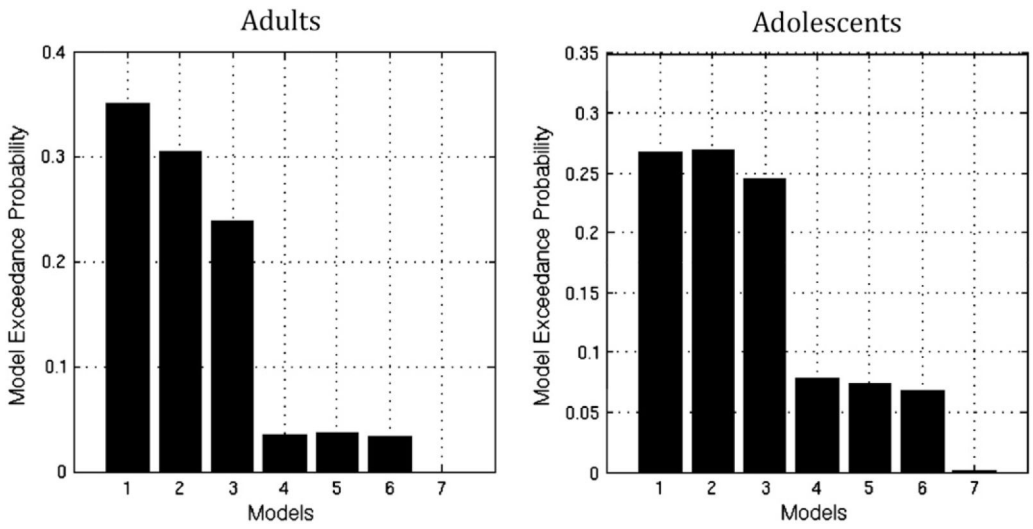

Fig. 6.

The exceedance probabilities resulting from Bayesian Model Selection (BMS) for the seven models hypothesized in Fig. 3. In both the adult (left) and adolescent (right) group, Models 1, 2, and 3 were similarly best-fit. See Table 4 for full list of exceedance probabilities.

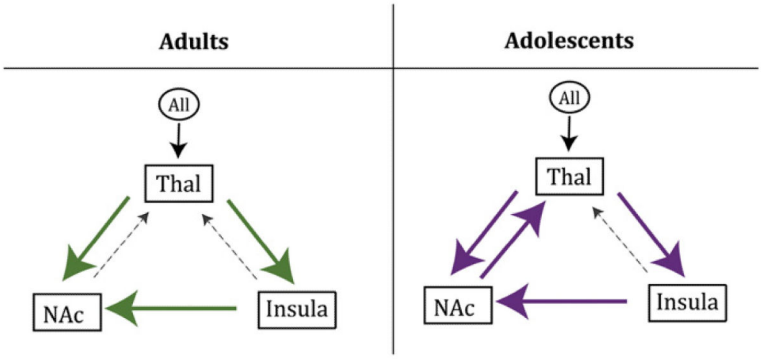

Fig. 7.

Significant endogenous connectivity in adults and adolescents. Endogenous connectivity refers to the connectivity between regions across the whole task, irrespective of cue phase. In color are those connections that were significant for each group, based on the best-fit, fully connected Model 1. Non-significant connections of Model 1 are shown with dashed, grey arrows. One-sample t-test, $p<0.05$.

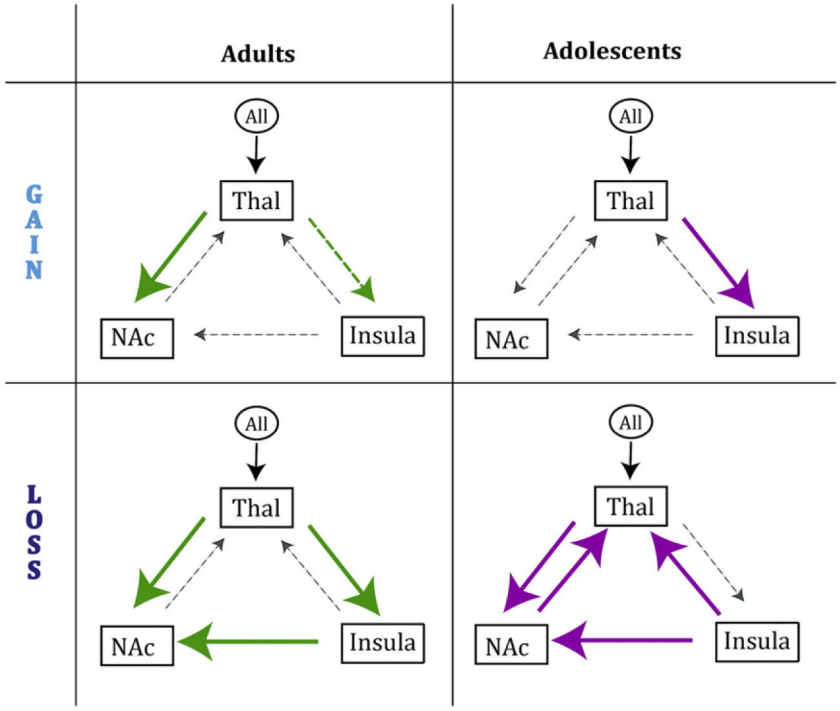

Fig. 8.

Significant modulation of the best-fit Model 1 connections by all gain or all loss cues in typical adults and adolescents. The connections significantly modulated by all gain or all loss cues are in color for each group. Non-significant connections are shown with dashed, grey arrows. One-sample t-test, $p<0.05$. A colored, dashed line indicates trend towards significance.

Table 1A

All gain cues vs. neutral cue: peak voxels for regions commonly activated in previous studies of the Monetary Incentive Delay (MID) task. Peak voxels within anatomic masks of each region are reported for the contrast all gain cues vs. the neutral cue. Reported peak voxels for thalamus and insula are restricted to anatomic subdivisions of interest–anteromedial thalamus and anterior insula, respectively–that were used for DCM. Small-volume corrected p<0.05, family-wise error (FWE). MNI coordinates.

	Adults			Adolescents		
	p-value	T-score	x,y,z	p-value	T-score	x,y,z
Nucleus accumbens (r)	< 0.001	6.31	16,16, −4	0.001	4.97	10,12, − 4
Nucleus accumbens (l)	0.001	4.71	− 10,14, − 2	0.001	4.76	− 6,14, 0
Insula (r)	0.004	5.1	32, 22, −8	0.028	3.74	34, 20, − 6
Insula (l)	0.031	4.06	−30, 24, 8	0.001	5.56	− 28,14, −4
Thalamus (r)	<0.001	5.47	8, 0, 6	0.016	3.79	4, −14, 6
Thalamus (l)	<0.001	5.51	−4, −12,8	0.021	3.63	− 6, 0, 6
Putamen (r)	<0.001	6.99	20,10, −2			
Putamen (l)	<0.001	8.38	−22, 0,10	0.008	4.43	18, 6, −12
Caudate (r)	<0.001	5.88	12,12,0	0.011	4.23	10,12,0
Caudate (l)	0.001	5.03	−10,12,2	0.005	4.51	− 8,14, 2
Amygdala (r)	0.009	3.82	28, −2, −10	0.019	3.63	20, 0, −14
Amygdala (l)	0.007	3.9	−20, 2, −12	0.001	4.81	−18, 2, −14
Anterior cingulate cortex (r)	0.004	4.83	6,10,44			
Anterior cingulate cortex (l)	0.022	4.18	− 4, 4, 44			
Motor cortex (r)	0.036	4.13	2 4, −18, 66			
Motor cortex (l)	<0.001	7.25	−38, −6,54	0.025	4.53	− 40, −16, 58
Premotor cortex (r)	0.001	5.45	2, − 2, 58			
Premotor cortex (l)	<0.001	6.33	−6, −4, 56			

Table 1B

All gain cues vs. neutral cue: Between-group analysis of peak voxels for regions com monly activated in previous studies of the Monetary Incentive Delay (MID) task. Peak voxels within anatomic masks of each region are reported for the contrast all gain cues vs. the neutral cue. Small-volume corrected $p < 0.05$, family-wise error (FWE). MNI coordinates.

	Adults > Adolescents			Adolescents > Adults		
	p-value	T-score	x,y,z	p-value	T-score	x,y,z
Putamen (r)	0.044	3.30	26, −4,12			
Motor cortex (l)	0.030	3.95	−38, −4,56			

Table 2A

All loss cues vs. neutral cue: Peak voxels for regions commonly activated **in** previous studies of the Monetary Incentive Delay (MID) task. Peak voxels within anatomic masks of each region are reported for the contrast all loss cues vs. the neutral cue. Reported peak voxels for thalamus and insula are restricted to anatomic subdivisions of interest–anteromedial thalamus and anterior insula, respectively–that were used for DCM. Small-volume corrected p<0.05, family-wise error (FWE). MNI coordinates.

	Adults			Adolescents		
	p-value	**T-score**	**x,y,z**	**p-value**	**T-score**	**x,y,z**
Nucleus accumbens (r)	< 0.001	5.25	12,14, −2	0.012	3.61	10,10, −6
Nucleus accumbens (l)	0.004	4.01	−12,12, −6	0.008	3.85	−6,16,0
Insula (r)	0.002	5.33	32, 26, −6			
Insula (l)						
Thalamus (r)	0.018	3.55	8, −12,6	0.019	3.61	2, 0, 10
Thalamus (l)	0.023	3.45	− 8, 0, 4	0.042	3.21	−6, 0, 10
Putamen (r)	<0.001	7.51	26, 2, 2			
Putamen (l)	0.002	4.76	−16, 6,0			
Caudate (r)	<0.001	5.38	12,12,0			
Caudate (l)	0.020	3.75	−10,12,0	0.022	3.79	−4, 8, 14
Amygdala (r)	0.027	3.32	28, − 4, −10			
Amygdala (l)	0.037	3.13	−18, 2, −12	0.008	3.85	−6,16,0
Anterior cingulate cortex (r)	0.013	4.36	4, − 2, 48			
Anterior cingulate cortex (l)	0.003	5.03	− 4, 4, 44			
Motor cortex (r)	0.001	5.77	2 44, − 6, 50			
Motor cortex (l)	<0.001	6.03	−36, −12, 58	0.025	4.47	−42, −16,54
Premotor cortex (r)	<0.001	6.04	2, − 2, 56			
Premotor cortex (l)	<0.001	6.07	− 4, − 4, 56			

Table 2B

All loss cues vs. neutral cue: Between-group analysis of peak voxels for regions com monly activated in previous studies of the Monetary Incentive Delay (MID) task. Peak voxels within anatomic masks of each region are reported for the contrast all loss cues vs. the neutral cue. Small-volume corrected $p<0.05$, family-wise error (FWE). MNI coordinates.

	Adults > Adolescents			Adolescents > Adults		
	p-value	T-score	x,y,z	p-value	T-score	x,y,z
Putamen (r)	0.005	4.08	26, 0, 0			

Table 3A

All cues vs. neutral cue: Peak voxels for regions commonly activated in previous studies of the Monetary Incentive Delay (MID) task Peak voxels within anatomic masks of each region are reported for the contrast all cues vs. the neutral cue. Reported peak voxels for thalamus and insula are restricted to anatomic subdivisions of interest–anteromedial thal amus and anterior insula, respectively–that were used for DCM. Small-volume corrected p<0.05, family-wise error (FWE). MNI coordinates.

	Adults			Adolescents		
	p-value	T-score	x,y,z	p-value	T-score	x,y,z
Nucleus accumbens (r)	< 0.001	4.44	14,14, −4	0.002	4.53	10, 10, −6
Nucleus accumbens (l)	0.002	6.09	−10,14, −2	0.001	4.69	− 6,16,0
Insula (r)	0.001	5.38	32, 24, −8	0.033	3.63	36, 18, −8
Insula (l)	0.027	4.12	−32, −28,16	0.002	5.00	− 28,16, − 2
Thalamus (r)	0.002	4.51	8, −12,6	0.041	3.25	4, −12,8
Thalamus (l)	0.002	4.65	−4, −14,6	0.02	3.63	− 6, 2, 8
Putamen (r)	<0.001	7.77	26, 2, 2	0.028	3.81	18, 10, −8
Putamen (l)	<0.001	6.85	−22, 0,10	0.017	4.04	18, 6, −12
Caudate (r)	<0.001	6.03	12,12,0	0.039	3.60	10, 12,0
Caudate (l)	0.002	4.65	−10,12,2	0.007	4.37	− 6,14,4
Amygdala (r)	0.009	3.83	28, −4, −10			
Amygdala (l)	0.006	3.95	−18, 2, −14	0.006	4.1	−18, 2, −14
Anterior cingulate cortex (r)	0.007	4.63	4, 0, 48			
Anterior cingulate cortex (l)	0.032	4.01	− 4, 4, 44			
Motor cortex (r)	0.003	5.24	42, − 8, 46			
Motor cortex (l)	<0.001	6.83	−38, −6,54			
Premotor cortex (r)	<0.001	6.29	2, − 2, 58			
Premotor cortex (l)	<0.001	6.8	−6, −4, 56			

Table 3B

All cues vs. neutral cue: Between-group analysis of peak voxels for regions commonly activated in previous studies of the Monetary Incentive Delay (MID) task. Peak voxels within anatomic masks of each region are reported for the contrast all cues vs. the neu tral cue. Small-volume corrected $p<0.05$, family-wise error (FWE). MNI coordinates.

	Adults > Adolescents			Adolescents > Adults		
	p-value	T-score	x,y,z	p-value	T-score	x,y,z
Putamen (r)	0.007	4.00	26,0,0			
Anterior cingulate cortex (l)				0.045	3.63	− 2, 42, − 2

Table 4

Exceedance probabilities, for each model. All probabilities sum to one, indicating the relative fit of the model.

	Model 1	Model 2	Model 3	Model 4	Model 5	Model 6	Model 7
Adults	0.3270	0.3106	0.2499	0.0399	0.0365	0.0361	0
Adolescents	0.2918	0.2582	0.2324	0.0658	0.0747	0.0771	0

Table 5

Parameter weights representing the strength of endogenous connectivity of Model 1, with significant values in bold.

	Adults		Adolescents	
	Mean (Hz)±SEM	**t, sig.**	**Mean (Hz)±SEM**	**t, sig.**
Thai → NAc	**0.049 ± 0.019**	**t(29) = 2.53, p = 0.017**	**0.051 ±0.023**	**t(23) = 2.17, p= 0.041**
NAc → Thal	0.00020 ±0.0014	t(24) =−0.138, p = 0.89	**0.0032 ± 0.0014**	**t(20) = 2.33, p= 0.030**
Thai → Insula	**0.053 ±0.014**	**t(29) = 3.85, p = 0.001**	**0.049± 0.021**	**t(23) = 2.37, p= 0.026**
Insula → Thal	−0.0011 ±0.0013	t(26) = − 0.87, p = 0.39	0.0010 ±0.0013	t(19) =0.794, p = 0.437
Insula → NAc	**0.0095 ±0.0029**	**t(29) = 3.30, p = 0.003**	**0.011 ±0.0039**	**t(23) = 2.85, p= 0.009**

Table 6

Modulation of Model 1 connections by gain or loss cues in the adult group. Those in bold were significantly influenced.

Adults	**All gain cues**		**All loss cues**	
	Mean (Hz)±SEM	**t, sig.**	**Mean (Hz)±SEM**	**t, sig.**
Thal → NAc	**0.018 ± 0.0073**	**t(26) = 2.44, p= 0.022**	**0.018 ± 0.0074**	**t(29) = 2.40, p = 0.023**
NAc → Thal	− 0.000017 ±0.00023	t(25) = − 0.076, p= 0.94	0.000060 ±0.00015	t(25) = 0.40, p = 0.69
Thal → Insula	0.0013 ±0.0067	t(28) = 2.033, p = 0.055	**0.015 ±0.0068**	**t(29) = 2.15, p = 0.04**
Insula → Thal	0.00006 ±0.00017	t(25) = 0.36, p= 0.72	−0.00048 ±0.0001	t(25) = −0.47, p = 0.65
Insula → NAc	0.0017 ±0.0013	t(26) = 1.26, p= 0.22	**0.00010 ± 0.00033**	**t(28) = 3.03, p = 0.005**

Table 7

Modulation of Model 1 connections by gain or loss cues in the adolescent group. Those in bold were significantly influenced.

Adolescents	**All gain cues**		**All loss cues**	
	Mean (Hz)±SEM	**t, sig.**	**Mean (Hz) ±SEM**	**t, sig.**
Thal → NAc	0.0057 ±0.0093	t(23) =0.61, p = 0.55	**0.031 ±0.011**	**t(23) = 2.87, p = 0.009**
NAc → Thal	0.00014 ±0.00016	t(20) =0.85, p = 0.41	**0.00055 ±0.00018**	**t(21) = 3.01, p = 0.007**
Thal → Insula	**0.026± 0.010**	**t(23) = 2.57, p= 0.017**	0.016 ±0.010	t(23) = 1.63, p = 0.12
Insula → Thal	0.00041 ±0.00026	t(20) = 1.58, p = 0.13	**0.00058 ±0.00024**	**t(23) = 2.41, p = 0.024**
Insula → NAc	0.00021 ±0.00019	t(21) = 1.07, p = 0.30	**0.00083 ± 0.00031**	**t(21) = 2.65, p = 0.015**